

# A comparison of four methods to map biomass from Landsat-TM and inventory data in western Newfoundland

S. Labrecque<sup>a</sup>, R.A. Fournier<sup>a,\*</sup>, J.E. Luther<sup>b</sup>, D. Piercey<sup>b</sup>

<sup>a</sup> Centre d'Applications et de Recherches en Télédétection (CARTEL), Université de Sherbrooke, 2500 boul. de l'Université, Sherbrooke, Qué., Canada J1K 2R1

<sup>b</sup> Natural Resources Canada, Canadian Forest Service, Atlantic Forestry Centre, P.O. Box 960, Corner Brook, Newfoundland and Labrador, Canada A2H 6J3

Received 6 July 2005; received in revised form 20 January 2006; accepted 21 January 2006

## Abstract

Spatial measures of forest biomass are important to implement sustainable forest management, monitor global change, and model forest productivity. Several methods for estimating forest biomass by remote sensing have been developed, but their comparative advantages have not been evaluated for large areas in Canada. This study compares four methods to map forest biomass on an extended pilot region (20,000 km<sup>2</sup>) located in western Newfoundland. The methods include: (i) Direct Radiometric Relationships (DRR), (ii) *k*-Nearest Neighbors (*k*-NN), (iii) Land Cover Classification (LCC), and (iv) Biomass from Cluster Labeling Using Structure and Type (BioCLUST). The results of each method were evaluated using an independent set of ground survey plots and compared with a baseline biomass map generated from biomass tables applied to forest inventory stand maps. Considering the root mean square error (RMSE) assessed with the inventory plots, the DRR, *k*-NN, and BioCLUST methods provided similar results, with average RMSE values of 59, 59, and 58 t/ha, respectively. Bias values were lowest for the *k*-NN method followed by DRR, BioCLUST, and LCC (6, –8, 17, and 42 t/ha, respectively). Assessed with the baseline map, the BioCLUST method produced the lowest RMSE (41 t/ha) and bias (–4 t/ha) followed by the DRR and *k*-NN methods, with RMSE values of 47 and 54 t/ha and bias values of 9 and 23 t/ha, respectively. The method using biomass tables applied on the classified TM image (LCC) provided the greatest RMSE and bias, but may be suitable for applications that do not require a high level of precision. The BioCLUST and LCC methods provided practical advantages for the type of data sets available. Overall, the choice of a method rests on both the availability of data sets and the level of precision of the results required.

Crown Copyright © 2006 Published by Elsevier B.V. All rights reserved.

**Keywords:** Forest biomass; Mapping; Landsat-TM; Remote sensing

## 1. Introduction

The need for reliable monitoring of forest biomass is increasingly important, in particular to support requirements related to sustainable forest management and carbon accounting. Planning and managing of forest operations for commercial use or the study of ecosystem productivity both require biomass mapping (Parresol, 1999). Estimating biomass is also a good way to measure the potential energy of a forest, because plant material (biomass) stores the solar energy needed for photosynthesis (Bérard, 1996). Because forests play an important role in the carbon cycle, radiation budget, and in maintaining climatic

balance, variation in biomass quantity can be a good indicator of changes in these processes (Roy and Ravan, 1996). Moreover, since the Kyoto protocol on greenhouse gas emission reduction, forests have been targeted for reducing carbon emissions because they store great quantities of carbon and exchange it with the atmosphere through photosynthesis and respiration (Brown et al., 1999). The quantities of carbon released into the atmosphere by forests are greatly increased by deforestation, changes in land use, and natural disturbances (e.g., fire), whereas regrowth tends to increase carbon storage in the vegetation. Forest management can, therefore, help in attaining a favorable carbon account by increasing the forested area (Brown et al., 1996). The ability to map forest biomass is thus important for monitoring changes in forest structure and changes in the carbon account.

Traditional methods of estimating forest biomass at the tree level use allometric equations, developed as a function of the

\* Corresponding author. Tel.: +1 819 821 8000x3209; fax: +1 819 821 7944.

E-mail address: [Richard.Fournier@USherbrooke.ca](mailto:Richard.Fournier@USherbrooke.ca) (R.A. Fournier).

species and such characteristics as tree height and diameter at breast height (DBH). These methods are time consuming and expensive, and the equations are specific to the location of the sample plots used for their development, and may not necessarily be applicable to other regions (Hall et al., 2002). Scaling biomass estimates up to the stand level depends on stand-level forest inventories and the date of the inventory (Fournier et al., 2003). Monitoring environmental variables requires a shorter temporal resolution than is currently available from typical forest inventories, which are usually repeated over 10-year intervals in Canada. Methods to map forest biomass are greatly needed at spatial resolutions compatible with forest inventory management and with finer temporal resolution than current inventory cycles.

Landsat Thematic Mapper (TM) imagery is a practical product for developing biomass mapping methods because of: (i) the continuity of the Landsat program since the 1970s, (ii) the relevance of the TM and ETM+ spectral bands of its sensors, and (iii) the suitable spatial resolution for regional mapping (i.e., 30 m for TM/ETM+ multispectral). The six bands of Landsat TM are distributed in regions of the spectrum that are sensitive to vegetation amount. Cohen and Spies (1992) have compared the spatial and spectral performances of Landsat TM and SPOT HRV and they concluded that, if only spectral information is considered, TM data are more useful than HRV for estimating forest structure, even if the latter has a higher spatial resolution. Moreover, Lefsky et al. (2001) evaluated the performances of five sensors (Landsat TM, Landsat TM multitemporal, AVIRIS, ADAR, and a LiDAR sensor) for the estimation of eight forest stand attributes in a Douglas-fir (*Pseudotsuga menziesii*) forest. They suggested that the use of two sensors to incorporate higher spatial and spectral resolution (e.g., ADAR and AVIRIS) did not significantly improve the prediction of stand attributes.

Although many methods exist for mapping forest biomass, their relevance in contexts other than those for which they were tested is difficult to assess. The weakness of some methods stems from their limited ability to be applied over large areas. Another consideration of many satellite-driven methods is their exclusive focus on the spectral information, thus leaving out the spatial and temporal dimensions. Moreover, some methods may provide satisfactory results in certain contexts, but their applicability in the Canadian context is unknown. The objective of this study is to evaluate methods to estimate aboveground forest biomass from remotely sensed data, and assess their relative advantages and disadvantages for large-scale implementation in Canadian forests. In this paper, forest biomass refers to the oven-dry weight of all aboveground material from trees with a DBH > 1 cm.

## 2. Biomass mapping methods

Methods available for mapping forest biomass fall under two main approaches: those using radiometric modeling and those linking a conversion table to a thematic classification of the image. Radiometric methods have been widely used, and entail regression analysis to link spectral values to measured or

estimated biomass at corresponding locations (Franklin, 1986; Roy and Ravan, 1996; Jakubauskas and Price, 1997; Foody et al., 2003). The spectral values can be the digital numbers or their radiometric transformations (e.g., radiance at the top of the atmosphere, surface reflectance) recorded in each image channel, as well as band ratios and vegetation indices. Studies have had variable results for defining the most useful band or indices to map biomass and other parameters, and have been inconclusive for suggesting a consistent relationship (Franklin, 1986; Cohen and Spies, 1992; Roy and Ravan, 1996; Jakubauskas and Price, 1997; Gerylo et al., 2002; Dong et al., 2003). Moreover, each application requires an assessment of the optimal bands and indices for estimating biomass from spectral relationships.

Non-parametric mapping is another radiometric method that relies on *k*-Nearest Neighbors, or *k*-NN (Fazakas et al., 1999; Tomppo et al., 1999; Tokola, 2000; Franco-Lopez et al., 2001; Reese et al., 2002). This method makes no assumptions about the distributions of the variables used for the classification (Franco-Lopez et al., 2001; Holmström, 2001) and is based on two important premises. First, the pixel values of an image depend only on the forest condition, and not on the geographic location (Fazakas et al., 1999). Second, the ground sample plots are distributed over a large area (e.g., the surface covered by a satellite image), and can be used as truth data for estimating the remaining image surface (Tokola et al., 1996; Franco-Lopez et al., 2001). Where there is a good representation of ground sample plots, this method has performed well for biomass estimation, and as a result is widely used in Finland and Sweden (Fazakas et al., 1999; Reese et al., 2002).

The second approach uses biomass conversion tables applied to a thematic classification of the satellite image. This method is similar in principle to the application of biomass or volume tables to forest polygons mapped by airphoto interpretation and contained in traditional forest inventories (Penner et al., 1997; Fournier et al., 2003). The classification can be done to any level of thematic detail as long as the conversion tables match the thematic classes. Intuitively, the level of precision of the resulting biomass map will likely depend on the level of detail of the classification. For example, a broad classification of land cover (Wulder et al., 2003), would be expected to give a coarse representation of biomass where biomass values would be assigned to broad land cover classes (for example, conifer (C), deciduous (D), or mixed (M) stands with varying levels of crown closure (open, sparse, and dense).

As part of a national strategy for biomass estimation in Canada (Luther et al., 2002), a practical method for large-scale mapping of forest biomass using a more detailed classification of cover types or forest species was developed (Luther et al., in press). The method, Biomass from Cluster Labeling Using Structure and Type (BioCLUST), consists of a suite of procedures that involve: (i) hyperclustering a Landsat-TM image, (ii) semi-automatic labeling of the resulting clusters with forest type and structural information, and (iii) applying stand-level models derived from field plots, which predict biomass as a function of height and crown closure within forest species type classes. The BioCLUST method takes advantage of existing forest inventory systems to optimize the character-

ization of spectral clusters with forest type and structure information that is subsequently used for biomass estimation. BioCLUST was developed as an alternative method to other biomass mapping methods (e.g., Direct Radiometric Relationships and  $k$ -NN) when scene-specific data requirements cannot be met. The thematic level of detail of the BioCLUST method corresponds to regional conversion tables developed by Fournier et al. (2003).

The methods selected for comparison in this study included (Fig. 2): (i) Direct Radiometric Relationships (DRR), linking spectral values to measured biomass at plot locations, (ii)  $k$ -NN estimation and mapping of biomass using inventory plots, (iii) Land Cover Classification (LCC), with application of biomass conversion tables, and (iv) BioCLUST classification and use of forest structure and type for biomass mapping. We felt that these four methods represented a spread of the most suitable candidates for large-scale mapping of forest biomass in Canada. In that context, the relative advantages and disadvantages of implementation were compared.

### 3. Methods

#### 3.1. Test area

The test area selected for this study is located in western Newfoundland near Corner Brook and Deer Lake (Fig. 1). It is about 20,000 km<sup>2</sup> of area and encompasses parts of three

ecoregions (Government of Newfoundland and Labrador, 2003): southwestern Newfoundland, central Newfoundland and the Long Range Mountains. The northern boundary of the region is the southern limit of Gros Morne National Park (Lat. 49°30'). Hills and undulating terrain characterize the topography of the eastern part. Elevation varies between 0 and 725 m, with a mean slope inclination between 0 and 20° and extremes values up to 60°.

The ecosystems within the test area are favorable to forest growth, having some of the most productive stands in Newfoundland. The forest covers nearly 40% of the territory, largely dominated by balsam fir (*Abies balsamea*) and black spruce (*Picea mariana*), with yellow birch (*Betula alleghaniensis*), red maple (*Acer rubrum*), and aspen (*Populus tremuloides*) also present. Higher elevation areas are primarily rocks and barren lands. Limestone till and slate are the dominant soil surface materials, with nutrient-poor coarse-textured till in the eastern part. The region's climate is humid, with significant snowfall in winter (>4 m/year in high-elevation areas).

#### 3.2. Inventory plot database

The ground data were forest inventory permanent and temporary sample plots (PSP and TSP, respectively) from the provincial Department of Forest Resources and Agrifoods (DFRA) of the Government of Newfoundland and Labrador

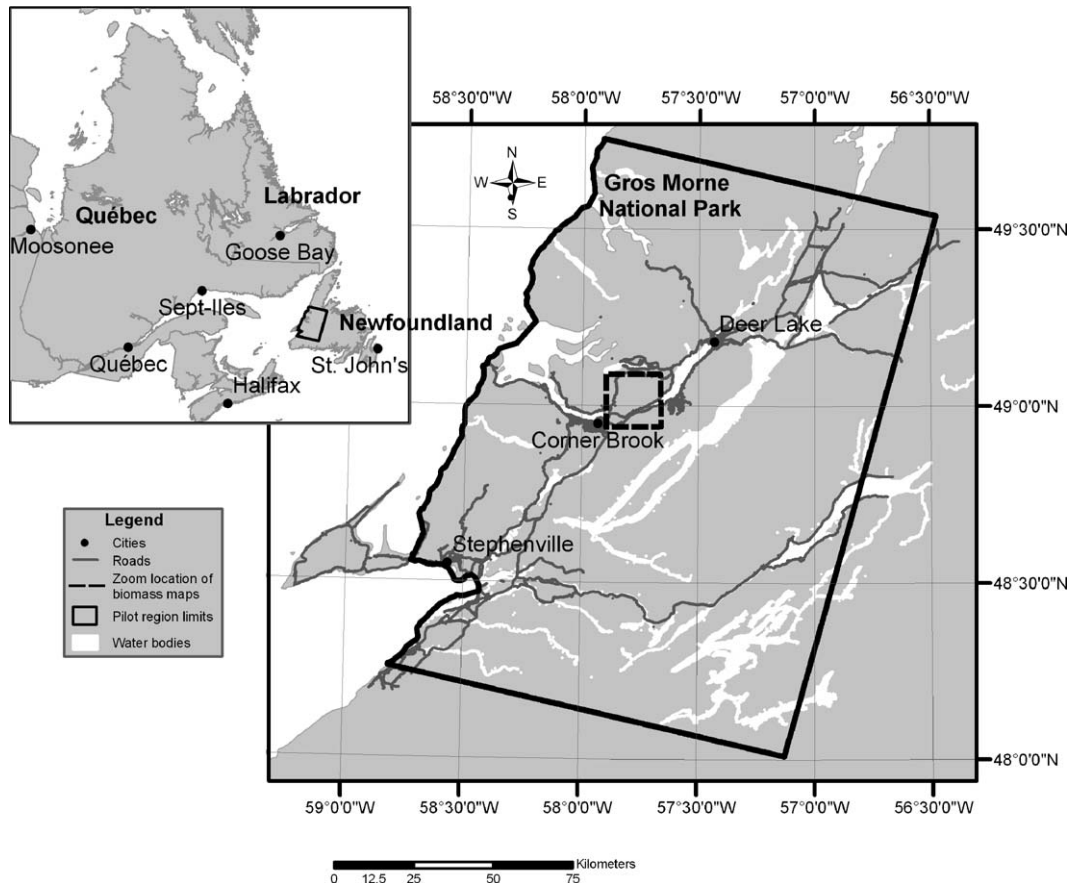


Fig. 1. Location of the test area.

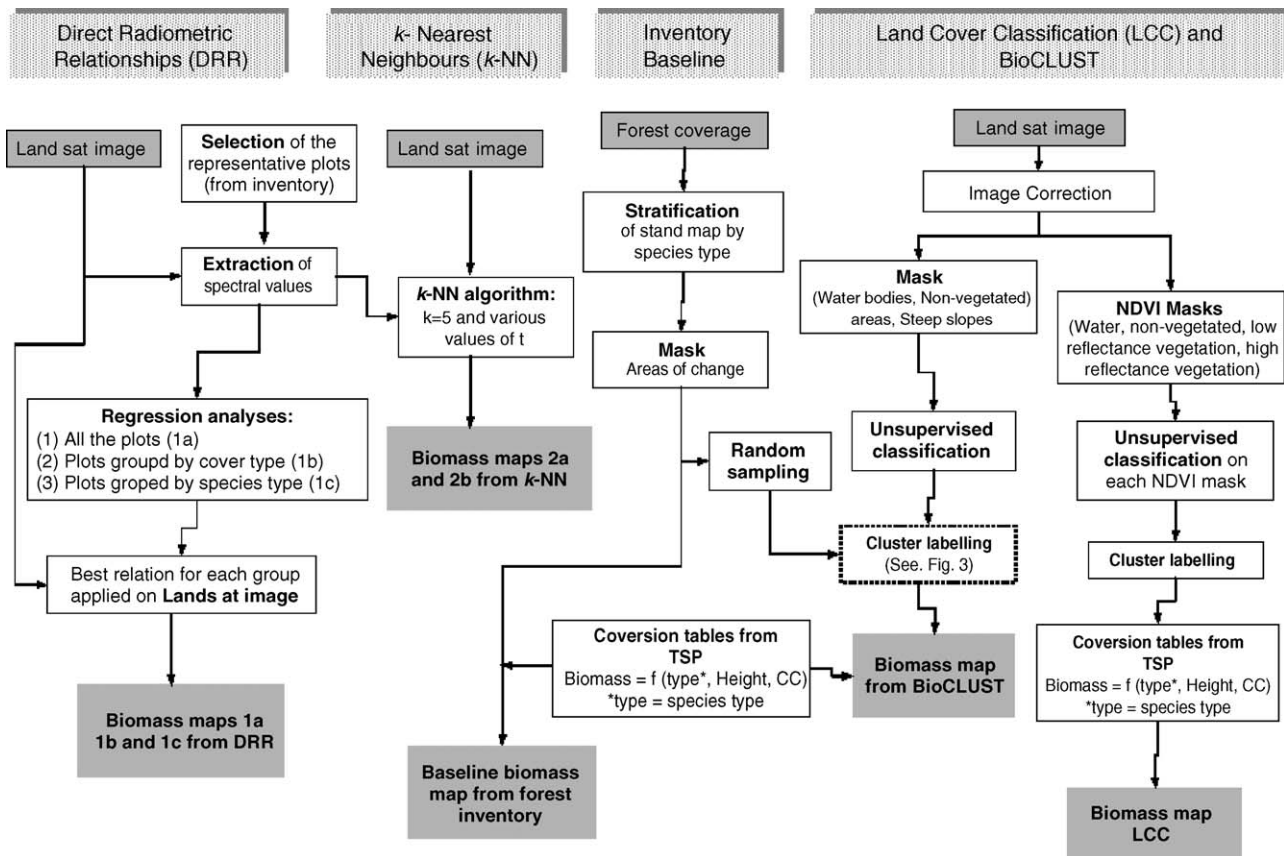


Fig. 2. Flow diagram of the procedures used in the four biomass mapping methods from Landsat TM and forest inventory data (adapted from Guindon et al., 2002).

(NL). Measurements were made between 1975 and 1995. The plots have an area of 200 m<sup>2</sup> and were distributed using a stratified random procedure, located only in productive forest areas. Species height and DBH were recorded for all the trees with a DBH > 9 cm. For smaller trees (height 1–9 cm), these parameters were recorded in a subplot located in the plot. For each plot, stand characteristics such as species composition, age class, crown closure class, dominant tree height class, and site index were also estimated (Fournier et al., 2003). Biomass values of these plots were estimated from tree level equations (Lavigne, 1982), thus providing the total dry weight of all live trees with a DBH > 1 cm. The plots were georeferenced and structured in a geographic information system (GIS) database.

Plots that were located in a stand where a disturbance (e.g., blowdown, insect defoliation, total or partial cut) occurred between the time of plot measurement and the acquisition of the TM image were considered unrepresentative of the database and removed. These adjustments reduced the number of non-representative plots or plots with a large temporal gap compared with the time of image acquisition. Plots were also removed if the spectral variability of the target and surrounding pixels was high. In such circumstances, the plot was not considered to be representative of its surroundings, either because of (i) its location at the edge of another stand, (ii) other landscape elements (e.g., road, river), (iii) high spatial variability within the stand, or (iv) geolocation error. The variability was calculated for a 3 × 3 pixel window centered at

each plot. Coefficients of variation were calculated for each plot and the threshold for removing the plots was set to 13.5% because it eliminated the most heterogeneous plots, but at the same time kept a sufficient number of plots in the database for analysis. The plots retained in the database were then enhanced by adding the spectral values of the six TM channels for windows of 1 × 1 pixel and 3 × 3 pixels.

Of the 1106 plots available for this study, 920 were retained for further analysis. A two-level hierarchy of surface cover was applied to the plots: (i) a stratification of conifer (C), deciduous (D), and mixed (M) stands, hereafter referred to as a forest cover type stratification and (ii) a further subdivision into five groups corresponding to species type groups, hereafter referred to as species type stratification including: balsam fir (bF), black spruce (bS), hardwood/softwood (hS), softwood/hardwood (sH) and white birch (*Betula papyrifera*) (wB—primarily white birch with some aspen). A compilation of the total number of plots in each group showed that conifer (72%) and balsam fir (54%) plots largely dominate the plot database compared with the other groups (mixed stand: 22.9%, deciduous: 6%, black spruce: 18%, softwood/hardwood: 15%, hardwood/softwood: 7%, and white birch: 6.7%).

From the final database, 70% of the plots (i.e., 644) were randomly selected as training data for the development of biomass mapping methods, and the remaining plots were kept for validation. The 276 validation plots were used to analyze the accuracy of the models derived from all the methods tested.

### 3.3. Inventory stand maps

The DFRA also provided digital maps of the forest stands of the pilot region interpreted from 1:12,500 aerial photographs acquired between 1986 and 1989. These maps contained information on the species composition, height class, crown closure, and type and year of disturbance.

The original labeling of the stand by the DFRA interpreters suggested 794 different stand species compositions exist within the test area. The forest stand composition was reduced into the two sets of stand composition stratifications, species types (balsam fir, black spruce, hardwood/softwood, softwood/hardwood, and white birch) and forest cover types (conifer, deciduous, and mixed stand), for compatibility with the satellite imagery and the results with the other methods tested. In addition, these divisions were compatible with working simplifications currently used by the DFRA and the Canadian National Forest Inventory (NFI), respectively. A compilation of the stand maps in the test area showed that 90.9% of the forested area was accounted for in this simplified stand composition. For the forested area, the species type stratification was dominated by balsam fir (64.9%), followed by black spruce (21.5%), softwood/hardwood (8.4%), hardwood/softwood (3.4%), and white birch (1.8%). The proportions are therefore 86.4%, 11.8%, and 1.8%, respectively, for the conifer, mixed stand, and deciduous classes.

### 3.4. Satellite image

A Landsat-5 TM scene collected on August 4, 1995 (path 5; row 26) was orthorectified with a digital elevation model (created from elevations of the 1:50,000 National Topographic Database), radiometrically corrected to transform digital numbers into reflectance at the top of the atmosphere (R. Landry, Canada Centre for Remote Sensing, personal communication), georeferenced in the same projection as the sample plots (UTM, Nad 83, zone 21N), and resampled at a spatial resolution of 25 m. The last step of the image preparation was to assign a cover type to each pixel of the Landsat-TM image. In the case of forested areas, both forest cover and species type stratifications were applied. The conifer/deciduous/mixed stand stratification was generated from a hyperclustering and labeling procedure (Wulder et al., 2003). In the case of the species type stratification, it was generated from the BioCLUST procedure (Luther et al., in press). The forest cover and species type layers generated by the classification procedures will be referred to in the remainder of this text as the

landbases needed to apply the different methods on the satellite image (i.e., cover type and species type landbases).

### 3.5. Biomass mapping methods

Fig. 2 shows the main steps of the four mapping methods.

#### 3.5.1. Direct Radiometric Relationships

Band ratios, vegetation indices, and tasseled cap components were calculated for pixels corresponding to the plot positions (Table 1). The spectral ratios and vegetation indices were calculated from the transformed image (at-sensor reflectance), but the tasseled cap transformations were calculated from the original pixel's digital number. Coefficients for the latter were published in Showengetdt (1997). Regression relationships were calculated between the spectral bands, band ratios, and vegetation indices (independent variables) and the predicted aboveground forest biomass. Linear, logarithmic, and second-order polynomial regressions were tested on the data. Regressions were made for all plots combined and also stratified by forest cover and species types. The regression analyses were performed on an individual pixel basis and for  $3 \times 3$  pixel windows. Multiple linear regressions were also tested to determine if a combination of several variables could improve the relationships. For each class, the best relationship derived: (i) without stratification of the plots, (ii) stratified by cover type, and (iii) stratified by species types was applied to the Landsat-TM image to produce biomass maps. Negative biomass values predicted by the regression equations were set to zero as negative biomass values are not possible in reality.

#### 3.5.2. *k*-Nearest Neighbors

The *k*-NN method applied here used the sample plots of the training data set as reference plots for a classification with the *k*-NN algorithm. Spectral values were extracted for each inventory plot according to its position on the satellite image, and the known values of a variable in the reference plots were then transferred to the pixels in the image that are the most spectrally similar and for which no variable values were known (Katila and Tomppo, 2001). The classification criterion of the *k*-NN is the minimum spectral distance computed between a pixel (*p*) of the image and a reference plot (*j*). The spectral distance can be weighted inversely proportional to the square distance (Fazakas et al., 1999; Tomppo et al., 1999), inversely proportional to the distance (Katila and Tomppo, 2001), or not weighted at all. The estimated biomass ( $\hat{e}$ ) of *p* was

Table 1  
Spectral information extracted from the Landsat TM-5 image

Bands	Vegetation indices	Band ratios	"Tasseled cap" transformations
TM1	NDVI		
TM2	$[(TM4 - TM3)/(TM4 + TM3)]$	TM4/TM3	Brightness (TC1)
TM3		TM5/TM4	Greenness (TC2)
TM4	NDMI	TM7/TM4	Wetness (TC3)
TM5	$[(TM4 - TM5)/(TM4 + TM5)]$		
TM7			

calculated by a weighted value of the biomass value ( $e_j$ ) of the  $k$  nearest reference plots, for each forested pixel of the image:

$$\hat{e}_p = \sum_{j=1}^k w_{j,p} \times e_{j,p} \quad (1)$$

where

$$w_{j,p} = \frac{1/d_{j,p}^t}{\sum_{i=1}^k 1/d_{i,p}^t} \quad (2)$$

and where  $d_{j,p}$  is the spectral distance between  $p$  and  $j$  (Reese et al., 2002).

In this study, two scenarios were tested. The first used an inverse square distance weighting function ( $t=2$ ) and  $k=5$ , and the second used the inverse distance weighting function ( $t=1$ ) with  $k=5$ . The value of  $k$  was chosen because earlier studies have shown that no real gain in accuracy was reached by using more than 10 neighbors, and that using a smaller number of  $k$  keeps the natural spatial variability and produces results with similar accuracies (Fazakas et al., 1999; Franco-Lopez et al., 2001; Katila and Tomppo, 2001; Reese et al., 2002). On the other hand, using fewer than five neighbors (i.e.  $k < 5$ ), has been found to decrease the accuracy and using too many neighbors ( $k > 10$ ) over generalizes the results (Tomppo et al., 1999; Reese et al., 2002). Two biomass maps were produced: one for each combination of  $k$  and weighting function.

### 3.5.3. Land Cover Classification

The LCC method used an available land cover map developed within the Earth Observation for Sustainable Development of Forests (EOSD) project, an initiative of the Canadian Forest Service and the Canadian Space Agency (Wood et al., 2002). The land cover map was produced using the same Landsat-TM image used in this study for assessing the four biomass mapping methods. The EOSD mapping procedures are described in detail in Wulder et al. (2003). In summary, an unsupervised classification was applied followed by spectral cluster labeling. The image pixels were first labeled in four broad categories using NDVI ranges: water, non-vegetated, low reflectance vegetation, and high reflectance vegetation. A  $K$ -means unsupervised classification algorithm was applied separately to the two sets

of pixels assigned as (1) low reflectance and (2) high reflectance. Each resulting spectral cluster associated with forested areas was labeled according to the land cover classes: conifer, deciduous, or mixed stands with three levels of crown closure (open, sparse, and dense). In this study, biomass values were assigned to each class of the Land Cover Classification from a conversion table (Table 2). The conversion table was developed using linear regression relationships that predict total aboveground biomass as a function of crown closure by cover type. The regional regression relationships were derived from biomass estimates for all TSP plots available for NL. As the EOSD project will be mapping land cover of all forested area in Canada, biomass mapping from this Land Cover Classification could be implemented at a national scale, provided that the biomass conversion tables are available on a regional basis.

### 3.5.4. Biomass from Cluster Labeling Using Structure and Type (BioCLUST)

For application of the BioCLUST method (Luther et al., in press), a  $K$ -means unsupervised classification algorithm was applied with parameters set to 240 clusters, exclusion threshold of 0.1 and 12 iterations. The clusters were labeled semi-automatically using information derived from forest inventory stand maps (Fig. 3). Fifty pixels were selected randomly for each forest stratum of the forest stand map, where the stratum was defined as a combination of the species type, and height and crown closure classes. This provided a representative set of unbiased samples for each stratum. The forest composition of each spectral cluster (%) was determined by overlaying the sampled layer with the clusters generated by the unsupervised classification. Biomass values were assigned to the clusters using the conversion table provided by Fournier et al. (2003), which provides aboveground biomass estimates for each species type as a function of height and crown closure. In Luther et al. (in press), the most frequently occurring stratum within each cluster was assigned the corresponding biomass value from the conversion table. In this study, a modified application of the conversion tables was tested. For each cluster, the final biomass value was calculated by multiplying the percentage of contribution of each height and crown closure class by the corresponding biomass value in the conversion tables, and then summing the results for the dominant species type.

Table 2  
Biomass lookup tables for the LCC method<sup>a</sup>

Cover type	$a$	$b$	$R^2$	RMSE	Density of crown closure		Predicted biomass (t/ha)
					Label	Midpoint (%)	
C	6.1704	0.6926	0.12	46.15	Dense	80.0	166.09
					Open	43.0	92.13
					Sparse	17.5	41.15
M	8.5028	0.6244	0.11	50.74	Dense	80.0	157.87
					Open	43.0	88.79
					Sparse	17.5	41.18
D	26.2810	0.3481	0.05	46.49	Dense	80.0	139.59
					Open	43.0	87.18
					Sparse	17.5	17.50

<sup>a</sup>Model form:  $a \times (\text{density midpoint})^b$ .

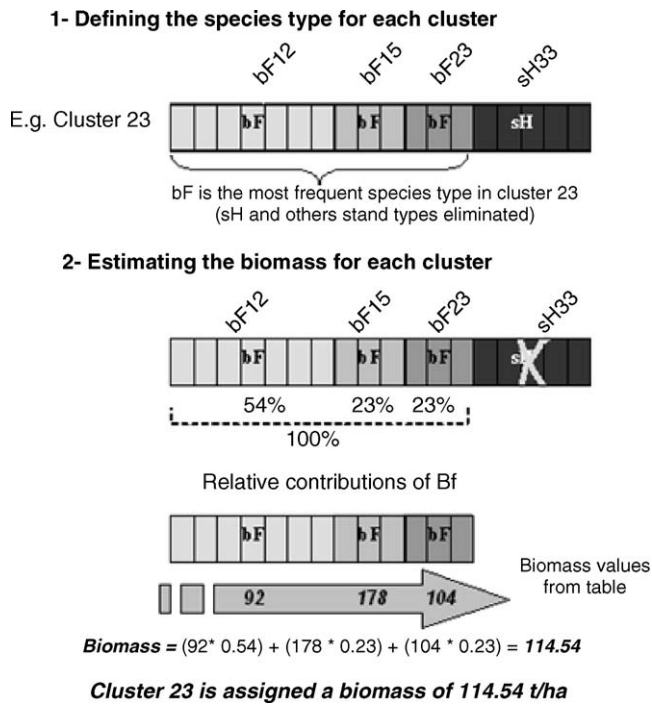


Fig. 3. BioCLUST procedure to assign biomass values to the spectral clusters.

### 3.6. Biomass error evaluation

The biomass maps produced by the four methods were compared based on the total biomass values and by values obtained for each cover and species type. This analysis indicates the variability of the methods by different forest types. Total biomass, mean biomass, and two error estimation indicators, i.e., RMSE (Eq. (3)) and bias (Eq. (4)), were calculated for each method.

$$\text{RMSE} = \sqrt{\frac{\sum_{i=1}^n (\hat{e}_i - e_i)^2}{n}} \quad (3)$$

where  $\hat{e}_i$  is the estimated biomass and  $e_i$  is the biomass value measured on the validation plots.

$$\text{Bias} = \bar{e}_1 - \bar{e}_2 \quad (4)$$

Table 3  
Evaluation of the baseline map using the validation plots

Group	<i>n</i> (plots)	Mean biomass from inventory plots (t/ha) <sup>a</sup>	Mean biomass from baseline map (t/ha) <sup>b</sup>	RMSE (t/ha)	Bias (t/ha)
bF	76	105	102	45	−3
bS	33	96	115	55	19
hS	14	121	89	68	−32
sH	30	129	106	62	−23
wB	16	106	93	45	−13
C	109	102	106	48	4
M	44	127	100	64	−27
D	16	106	93	45	−13
All	169	109	103	52	−6

<sup>a</sup> Mean biomass calculated using the biomass values in the field measurements database for the validation plots in the test area.

<sup>b</sup> Mean biomass values calculated using tables from Fournier et al. (2003) applied to the validation plots in the test area.

where  $\bar{e}_1$  is the mean value of the estimated biomass and  $\bar{e}_2$  is the mean value of the validation plots (Fazakas et al., 1999). In addition, the mean biomass and the corresponding standard deviations were calculated for ranges of 25 t/ha of biomass for each mapping method, allowing the determination of which biomass ranges are most sensitive to errors for each of the methods.

Two different sets of data were used as ground truth. First, the error evaluation was made from the validation plots that were randomly selected from the TSP/PSP database. These plots contain the most reliable information of the region, but they do not provide a good indication of the spatial distribution of biomass values. Second, the error assessment calculations were assessed with a baseline map. The baseline biomass map adopted in this study used the biomass conversion tables of Fournier et al. (2003) applied to the stand attributes of the forest inventory map. The resulting biomass map served as a reference map to compare the results from various methods and will hereafter be referred to as the baseline map. The choices made for a baseline map were guided by several reasons: (1) it is the best source of information available for the study area, (2) the stand map is generated by detailed interpretation from aerial photographs by experienced interpreters, and (3) biomass lookup tables applied on the forest stand maps are traditionally used for forest management purposes (e.g., volume estimation).

As the different methods used different landbases (i.e., the stand map for the baseline and the forest and species type stratifications for the four mapping methods), the biomass areas generated by the different methods were not identical. For comparison purposes, a mask was generated from all of the landbases. This mask represented the areas of overlap among the different biomass maps. The RMSE, bias and mean biomass values were calculated on the overlapping areas only.

## 4. Results and their interpretation

### 4.1. Baseline biomass from inventory

Total biomass and mean biomass values calculated for the baseline method in addition to the error estimations calculated from the validation plots (Table 3) provided an indication of the errors inherent in the baseline biomass map. These values

suggested that the baseline map underestimated biomass when compared with the validation plots, especially for mixed stands (hardwood/softwood, softwood/hardwood, and mixed stand), which had bias values ranging from  $-23$  to  $-32$  t/ha and a RMSE around 65 t/ha. All the species and forest cover type groups had negative bias, except for black spruce and conifer, and the bias calculated for the “All” category is  $-6$  t/ha. The lowest bias registered occurred for balsam fir. The RMSE values for the baseline ranged from 45 to 68 t/ha depending on the forest cover or species type and mean biomass estimated for the validation plots ranged from 89 to 115 t/ha. The contribution of balsam fir and black spruce to the total biomass was greater than those from all the other species types combined as they accounted for 85% of the total. Balsam fir accounted for almost 60% of the total biomass amount, and white birch stands accounted for only 2% of the total 44 Mt of biomass (Table 9).

#### 4.2. Biomass from DRR

The regressions with the highest  $R^2$  (Table 4) were generally obtained from the second order polynomial and the multiple linear regressions. The  $R^2$  values generally increased when using plots stratified by forest cover and species types compared with the results when using all the plots without stratification (Labrecque, 2004). When using the forest cover type stratification, the regressions applied to the conifer group provided the highest  $R^2$  of the three forest cover types. The regressions for coniferous (balsam fir and black spruce) and for mixed stands (hardwood/softwood and softwood/hardwood) species type resulted in higher  $R^2$  than plots with no stratification or with plots stratified by forest type. The use of the finest level of stratification helped improving  $R^2$  values, as well as the use of average spectral values calculated over windows of  $3 \times 3$  pixels. The brightness, greenness, and wetness components of the tasseled cap transformations, as well as TM1 and TM5 bands, were the most correlated to biomass of all the spectral values tested. Overall, the fits to a regression model were low for the western Newfoundland pilot region compared with the results of other studies. In addition, the bands or spectral values most correlated with biomass differed from other published studies. For example, Jakubauskas and Price (1997) found significant regression relationships

between biomass and TM7 ( $R^2 = 0.58$ ) and between biomass and NDVI ( $R^2 = 0.59$ ) in conducting multiple regressions for lodgepole pine (*Pinus contorta* var. *latifolia*) forests in Yellowstone Park. In our case, the highest  $R^2$  value obtained for multiple regressions was 0.160 for the black spruce group, which contained 113 plots, compared with 70 sample plots used by Jakubauskas and Price (1997).

The RMSE and bias (Table 5) were similar for the three levels of analysis, e.g., (1) with no stratification (all plots), and with stratification, (2) by forest cover type, and (3) by species type. The RMSE values for the “All” category were 54, 59, and 57 t/ha, respectively, when calculated using the validation plots, and 48, 47, and 50 t/ha, respectively, when calculated using the baseline map. The lower RMSE values obtained with the baseline map were probably due to the fact that biomass errors inherent in applying biomass conversion tables (Fournier et al., 2003) to the stand maps (Table 3) were not accounted for when the baseline was used as truth for validating the biomass maps derived from the image-based methods. For the same three levels of analysis, the overall bias values were 1,  $-8$ , and  $-2$  t/ha, respectively, when calculated using the validation plots, and 20, 9, and 18 t/ha, respectively, when calculated using the baseline. The RMSE and bias values calculated using the validation plots as “truth” suggest an underestimation of the biomass for the plots grouped by forest cover and by species type. However, when the baseline map is used as “truth”, black spruce is the group where biomass was most significantly underestimated. Bias values were lower when calculated from the validation plots because the baseline map already underestimated biomass. Consequently, the mean predicted biomass was higher for the best DRR models than those from the baseline map.

The range of RMSE values for the three DRR models calculated using the validation plots (47–83 t/ha from Table 5) were comparable but slightly higher than those of the baseline map (45–68 t/ha from Table 3). The same was also true for the bias values calculated using the validation plots for the DRR method ( $-24$  to 16 t/ha) and from the baseline map ( $-32$  to 19 t/ha). Mean biomass ranges from approximately 88 to 125 t/ha for the three levels of analysis. However, the relationships used for the forest cover type map gave the lowest total biomass (48 Mt in Table 9) compared with the DRR maps produced for the two other levels of analysis (52 and 53 Mt for “all plots”

Table 4  
Best relationships selected for the DRR method for three cases

Case	Group	n (plots)	Pixel vs. window	$R^2$	Model equation
One equation per species type	bF	365	(3 × 3)	0.097	$390.223 - 5.8124 (TC1) + 0.0291 (TC1)^2$
	bS	113	Pixel	0.155	$362.175 - 18.117 (TM4/3) - 8.939 (TM1) + 3.506 (TM7) + 145.17 (NDMI)$
	hS	42	(3 × 3)	0.124	$-329.14 + 8.2429 (TM4) - 0.0346 (TM4)^2$
	sH	86	Pixel	0.09	$334.483 - 1.251 (TC3) - 8.957 (TM2) + 1.478 (TC1) - 202.872 (NDVI)$
	wB	38	(3 × 3)	0.079	$642.846 - 5.991 (TM1) - 571.034 (NDMI) - 659.705 (TM7/4)$
One equation per forest cover type	C	478	(3 × 3)	0.096	$391.756 - 2.431 (TC3) - 11.252 (TM1) + 1.305 (TM5) + 102.996 (NDMI)$
	M	128	(3 × 3)	0.057	$130.381 + 2.530 (TM5) - 11.383 (TM2) + 4.886 (TM1)$
	D	38	(3 × 3)	0.079	$642.846 - 5.991 (TM1) - 571.034 (NDMI) - 659.705 (TM7/4)$
One equation for all the plots	Forested area	644	(3 × 3)	0.084	$346.982 - 0.299 (TC3) - 5.333 (TM3) + 4.573 (TM7) - 6.947 (TM1)$

Table 5  
Mean biomass, RMSE, and bias results for the DRR method

Case	Group	Plot values				Map values			
		<i>n</i> (plots)	Mean biomass (t/ha)	RMSE (t/ha)	Bias (t/ha)	<i>n</i> (pixels)	Mean biomass (t/ha)	RMSE (t/ha)	Bias (t/ha)
All the plots (1 equation)	bF	76	107	50	2	5,066,368	108	52	27
	bS	33	104	57	8	1,676,301	110	37	−0.16
	hS	14	125	71	4	276,137	116	39	22
	sH	30	113	52	−16	687,189	113	44	20
	wB	16	120	47	14	139,969	121	42	28
	C	109	106	53	4	6,742,969	108	49	20
	M	44	117	59	−10	960,326	113	42	20
	D	16	120	47	14	139,969	121	42	28
	All	169	110	54	1	7,842,964	109	48	20
Plots grouped by forest cover type (3 equations)	bF	76	96	55	−9	5,066,368	96	50	15
	bS	33	88	58	−8	1,676,301	96	40	−14
	hS	14	121	83	0.44	276,137	111	42	18
	sH	30	105	53	−24	687,189	104	46	11
	wB	16	122	53	16	139,969	121	47	28
	C	109	94	56	−8	6,742,969	96	47	8
	M	44	110	67	−17	960,326	106	45	13
	D	16	122	53	16	139,969	121	47	28
	All	169	101	59	−8	7,842,964	98	47	9
Plots grouped by species type (5 equations)	bF	76	103	53	−2	5,066,368	107	54	25
	bS	33	107	59	11	1,676,301	108	37	−2
	hS	14	119	64	−2	276,137	110	42	16
	sH	30	108	54	−21	687,189	107	47	14
	wB	16	117	65	11	139,969	114	43	22
	C	109	104	55	2	6,742,969	107	50	19
	M	44	111	57	−16	960,326	108	46	15
	D	16	117	65	11	139,969	114	43	22
	All	169	107	57	−2	7,842,964	107	50	18

Reporting is given for three cases representing different levels of stratification: (i) one equation derived from all the plots, (ii) three equations, one per forest cover type, and (iii) five equations, one for each of the species types.

and species type levels, respectively). Mean biomass was also slightly lower for the forest cover type map, but RMSE and bias were similar to the two other maps.

#### 4.3. Biomass from *k*-NN

The results from the application of the inverse square ( $t = 2$ ) and inverse ( $t = 1$ ) distance weighting function were similar (Table 6), indicating that the modification of this parameter did not have a significant impact on the results for our test area. In both scenarios, the number of neighbors ( $k$ ) was left at five. Total biomass was almost the same for the two scenarios (nearly 55 Mt for both) and mean predicted biomass was almost identical (results for the “All” category were 116 and 112 t/ha for both scenarios, using, respectively, validation plots and baseline map). The RMSE ranged from 37 to 81 t/ha for  $t = 1$  and from 37 to 85 t/ha for  $t = 2$  when using validation plots. The ranges of RMSE calculated using the baseline map were from 42 to 59 t/ha for  $t = 1$ , and from 43 to 59 t/ha for  $t = 2$ . Both scenarios suggested biomass overestimation: near 7 t/ha when using validation plots and 23 t/ha when using the baseline map. Only the softwood/hardwood species class and mixed wood forest class gave negative bias values and only when calculated using

the validation plots: for both scenarios, bias reached −12 t/ha for softwood/hardwood and −4 t/ha for mixed stand. The maximum range of RMSE and bias values calculated using the validation plots (RMSE: 37–85 t/ha, and bias: −12 to 19 t/ha) were comparable to those calculated for the baseline map (RMSE: 45–68 t/ha, and bias: −32 to 19 t/ha), but the total range differed.

Total biomass predicted by the *k*-NN method was higher than the one predicted by the baseline map, i.e., 55 and 44 Mt, respectively (Table 9). However, the relative contribution of each forest type was similar for each map: conifer: 85%, mixed stand: 13%, and deciduous: 2%. Mean biomass values calculated using the validation plots for the *k*-NN method (Table 6) were similar but slightly higher than those calculated for the baseline map (Table 3).

The RMSE values calculated using the validation plots were higher than those using the baseline map, especially for the black spruce, hardwood/softwood, and mixed stand classes. The opposite situation was noted for the calculation of bias values, i.e., values calculated using the validation plots were lower. In this case, almost all classes showed a strong difference between the bias calculated using the validation plots and the bias calculated using the baseline map, especially for the softwood/hardwood class, where the difference was about 35 t/ha.

Table 6  
Mean biomass, RMSE, and bias values for the *k*-NN method

Group	Plot values				Map values			
	<i>n</i> (plots)	Mean biomass (t/ha)	RMSE (t/ha)	Bias (t/ha)	<i>n</i> (pixels)	Mean biomass (t/ha)	RMSE (t/ha)	Bias (t/ha)
<i>k</i> -NN, <i>t</i> = 1								
bF	76	111	54	6	5,066,368	111	59	29
bS	33	114	68	18	1,676,301	111	42	1
hS	14	135	81	14	276,137	119	46	26
sH	30	117	57	-12	687,189	115	51	23
wB	16	119	37	13	139,969	124	49	31
C	109	112	58	10	6,742,969	111	55	22
M	44	123	66	-4	960,326	116	49	23
D	16	119	37	13	139,969	124	49	31
All	169	116	59	7	7,842,964	112	54	23
<i>k</i> -NN, <i>t</i> = 2								
bF	76	111	54	6	5,066,368	111	59	29
bS	33	115	67	19	1,676,301	111	43	1
hS	14	136	85	15	276,137	119	48	26
sH	30	117	57	-12	687,189	115	51	23
wB	16	118	37	12	139,969	124	50	31
C	109	112	59	10	6,742,969	111	56	22
M	44	123	67	-4	960,326	117	50	24
D	16	118	37	12	139,969	124	50	31
All	169	116	59	6	7,842,964	112	55	23

#### 4.4. Biomass from LCC

Total biomass provided by the LCC method was nearly 75 Mt (Table 9). The contribution of each forest type was similar to those found for the baseline map, i.e., conifer: 85%, mixed stand: 12%, and deciduous: 2%. Mean biomass values were high, ranging from 130 to 158 t/ha when using the validation plots and from 143 to 160 t/ha when using the baseline map (Table 7), whereas the mean biomass values for the “All” category were 89 and 103 t/ha when using the baseline map and the validation plots, respectively (Table 3). When using validation plots, RMSE and bias ranged from 54 to 87 t/ha and from 9 to 62 t/ha, respectively. Values were slightly different when using the baseline map: RMSE ranged from 63 to 85 t/ha and bias from 50 to 72 t/ha. Bias values suggest that this method strongly overestimated biomass because they were exceeding half of the RMSE values. When using validation

plots, the highest RMSE occurred for the coniferous classes (conifer, balsam fir, and black spruce) and for hardwood/softwood species class, whereas the lowest RMSE occurred for white birch species class. The RMSE values calculated using the validation plots for the LCC method (54–87 t/ha) were higher than those calculated for the baseline map (45–68 t/ha). Bias values for LCC (9–62 t/ha) were also much higher, and indicate only an overestimation of the biomass, by opposition with those found for the baseline map (-32 to 19 t/ha), which showed biomass overestimation or underestimation depending on the forest cover or species type.

#### 4.5. Biomass from BioCLUST

The BioCLUST method provided mean biomass values ranging from 85 to 102 t/ha when using the validation plots, and from 87 to 97 t/ha when using the baseline map (Table 8), with

Table 7  
Mean biomass, RMSE, and bias values for the LCC method

Group	Plot values				Map values			
	<i>n</i> (plots)	Mean biomass (t/ha)	RMSE (t/ha)	Bias (t/ha)	<i>n</i> (pixels)	Mean biomass (t/ha)	RMSE (t/ha)	Bias (t/ha)
bF	76	156	77	50	5,066,368	152	85	71
bS	33	158	87	61	1,676,301	159	63	49
hS	14	130	84	9	276,137	145	66	52
sH	30	147	69	17	687,189	149	72	56
wB	16	143	54	42	139,969	143	64	50
C	109	156	80	53	6,742,969	154	80	65
M	44	142	74	14	960,326	148	70	55
D	16	143	54	42	139,969	143	64	50
All	169	151	76	42	7,842,964	153	79	64

Table 8  
Mean biomass, RMSE, and bias values for the BioCLUST method

Group	Plot values				Map values			
	<i>n</i> (plots)	Mean biomass (t/ha)	RMSE (t/ha)	Bias (t/ha)	<i>n</i> (pixels)	Mean biomass (t/ha)	RMSE (t/ha)	Bias (t/ha)
bF	76	92	51	–13	5,066,368	92	44	11
bS	33	102	59	6	1,676,301	97	37	–13
hS	14	85	74	–36	276,137	89	30	–4
sH	30	90	69	–39	687,189	91	38	–2
wB	16	88	49	–18	139,969	87	27	–6
C	109	95	54	–7	6,742,969	93	42	5
M	44	88	70	–39	960,326	90	36	–3
D	16	88	49	–18	139,969	87	27	–6
All	169	93	58	–17	7,842,964	93	41	–4

Table 9  
Total biomass (tonnes) of the study area mapped by each method

Group	Baseline	Method						
		DRR, All plots	DRR, CDM	DRR, WG	<i>k</i> -NN, <i>t</i> = 1	<i>k</i> -NN, <i>t</i> = 2	LCC	BioCLUST
bF	25,648,547	34,077,782	30,359,326	33,616,415	34,898,326	34,845,640	48,143,219	29,099,982
bS	11,483,112	11,260,246	10,014,004	11,266,401	11,622,138	11,619,060	16,674,335	10,107,770
hS	1,589,852	1,966,024	1,887,566	1,865,968	2,028,477	2,030,017	2,471,974	1,515,312
sH	3,973,391	4,812,131	4,423,831	4,580,523	4,933,391	4,932,242	6,402,891	3,879,211
wB	808,032	1,056,673	1,055,096	996,358	1,076,802	1,078,950	1,247,463	758,937
C	37,131,659	45,338,028	40,373,330	44,882,816	46,520,464	46,464,700	64,817,554	39,207,752
M	5,563,243	6,778,155	6,311,397	6,446,491	6,961,868	6,962,259	8,874,685	5,394,523
D	808,032	1,056,673	1,055,096	996,358	1,076,802	1,078,950	1,247,463	758,937
All	43,502,934	53,172,856	47,739,823	52,325,665	54,559,134	54,505,909	74,939,702	45,361,212

overall mean values of 93 t/ha for both. Total biomass was near 45 Mt (Table 9). The RMSE values for the “All” category were 58 and 41 t/ha when using the validation plots and the baseline map, respectively. These results were similar to those of Luther et al., in press, where an overall RMSE of 64 t/ha (using the validation plots) and 45 t/ha (using the baseline map, referred to in Luther et al. as the photo-inventory map), although some variations were introduced in the BioCLUST method for this study.

The bias values indicated a slight tendency to underestimate biomass. Bias values calculated for the “All” encompassing category were –17 t/ha when using the validation plots and –4 t/ha when using the baseline map. Almost all classes had a negative bias, except for black spruce calculated using validation plots, and balsam fir and conifer calculated using the baseline map. The RMSE values of the baseline map ranged from 45 to 68 t/ha, which is comparable to the 49–74 t/ha range for BioCLUST when both were calculated using the validation plots. However, the BioCLUST method gave slightly lower biomass values for all classes of forest cover and species type. The RMSE values for BioCLUST were slightly higher than those found for the baseline map for all forest cover and species type. Bias of the black spruce species type (6 t/ha) is the only one to be lower than the bias of the baseline map (19 t/ha).

For the error calculation made using the validation plots, the highest and lowest RMSE values occurred for hardwood/softwood (74 t/ha) and white birch (49 t/ha), respectively,

whereas the greatest bias occurred for softwood/hardwood and mixed stand (–39 t/ha) and the least bias for black spruce (6 t/ha). For the error calculation made using the baseline map, the highest and lowest RMSE occurred for balsam fir (44 t/ha) and white birch (27 t/ha), respectively. The greatest and least bias values occurred for black spruce (–13 t/ha) and softwood/hardwood (–2 t/ha), respectively.

## 5. Discussion

### 5.1. Quantitative comparison of biomass mapping methods

The comparison of the RMSE values across methods provided an indication of the relative strength and weakness of each method. In general, the RMSE values of the four methods were slightly higher than those of the baseline map. There were some exceptions, where RMSE values from the satellite mapping method were lower, i.e., for softwood/hardwood of DRR and *k*-NN, and for white birch of *k*-NN. When using the validation plots, DRR, *k*-NN, and BioCLUST methods gave similar RMSE values of 59, 59, and 58 t/ha, respectively, for the “All” category, and LCC gave a higher value of 76 t/ha. Of the four methods, the deciduous class gave the lowest RMSE of the three forest cover types. The largest RMSE values for all methods came from the mixed stand class, except for the LCC method where conifer gave the highest value. When looking at the species type, the highest RMSE values were recorded by

hardwood/softwood for DRR, *k*-NN, and BioCLUST, and by black spruce for LCC. The white birch class provided the lowest values for all methods. Patterns are different when the baseline map is used instead of the validation plots for RMSE calculations. The RMSE values for DRR, *k*-NN, LCC, and BioCLUST were 47, 54, and 41 t/ha, respectively, for the “All” category, with a value of 79 t/ha for the LCC method. Lowest RMSE were recorded by mixed stand for DRR and BioCLUST, by mixed stand and deciduous for *k*-NN, and by deciduous for LCC. Highest RMSE were provided by conifer for *k*-NN, LCC, and BioCLUST, and by conifer and deciduous for DRR. When looking at the species type, the balsam fir class provided the greatest values for all methods. The lowest was recorded by softwood/hardwood for DRR, by black spruce for *k*-NN, and LCC, and by hardwood/softwood for BioCLUST. This comparison showed that the RMSE values calculated using the baseline map as “truth” were lower than the ones calculated using the validation plots.

A similar comparison of the bias values calculated using the validation plots showed that each method gave different results: values for the “All” category of  $-8$  t/ha for DRR,  $7$  t/ha for *k*-NN,  $42$  t/ha for LCC, and  $-17$  t/ha for BioCLUST. This suggested that *k*-NN and LCC methods tend to overestimate biomass slightly, whereas the DRR method may tend to underestimate it slightly. The BioCLUST method resulted in a biomass underestimation of about  $17$  t/ha, which was one of the highest values for all the methods. Bias values calculated using the baseline map provided different results, as almost all methods showed a biomass overestimation, except for the BioCLUST method, which slightly underestimated it by  $4$  t/ha. The results using the baseline map suggested that the BioCLUST method gave the least bias, followed by the DRR and by *k*-NN. The greatest bias was associated with the LCC method.

Tables 7 and 8 showed large differences between the RMSE and bias values of the LCC and BioCLUST methods. Both these methods used unsupervised classifications, cluster labeling, and biomass conversion tables, which could have led to more comparable results. However, the differences in the classification procedures and level of thematic stratification led to significant differences in results. The LCC method required manual labeling of spectral clusters applied to the map with two themes: cover types (conifer, deciduous, and mixed stand) and crown closure (three levels). In contrast, the BioCLUST method used semi-automatic labeling of spectral clusters applied to the map with three themes: species types (five types), crown closure (three levels), and height (eight levels). Overall, the BioCLUST method provided significantly better results compared with those from the LCC method for the test area.

The spatial distribution of biomass values in a map format permitted a comparison of the spatial patterns and variability from each method (Fig. 4). Biomass patterns were quite different depending on the method. First, all four methods, (DRR, *k*-NN, LCC, and BioCLUST) generated maps with pixel-level precision, whereas the baseline map was generalized over forest stand polygons. The resulting maps show higher variability on the maps made from the satellite image,

which is an advantage to address local heterogeneity in the biomass values. Second, the *k*-NN method was the only method that provided a good spatial distribution for all biomass ranges. Third, the map calculated from the LCC method showed a surprisingly high concentration of values in the range  $>150$  t/ha, which does not appear realistic for this test area. Furthermore, the high bias values in Table 7 associated with the LCC method also indicated biomass overestimation. In contrast, the map calculated from the BioCLUST method showed a relatively higher concentration of biomass value in the range  $75$ – $100$  t/ha when compared with the other methods. This suggested an overestimation of low biomass values and an underestimation of high values of biomass. Finally, the map resulting from the DRR method showed spatial distributions similar to those from the *k*-NN method. However, of all the methods, the LCC method appeared to be the one that made the strongest overestimation of the biomass values, with practically no biomass value lower than  $125$  t/ha.

The analysis of the results by ranges of  $25$  t/ha provided an indication how each method behaves in separate ranges of biomass and which ranges were most sensitive to errors (Fig. 5). Mean biomass values for each method were similar for the graphs generated using the baseline map (Fig. 5a) and using the validation plots (Fig. 5b) as “truth”. The mean values for the BioCLUST method were lower than for the other methods for biomass higher than  $100$  t/ha. This confirmed the underestimation of high biomass values that was suggested by Fig. 4. This pattern was not observed on the graph made using the validation plots because there were not enough plots in the  $125$ – $150$  t/ha and  $>150$  t/ha ranges to plot the results. For the mean and standard deviation (S.D.) values calculated using the baseline biomass values (Fig. 5a), each method gave low S.D. values ( $5$ – $8$  t/ha). An exception was found for the lowest and highest ranges, where the DRR and *k*-NN methods gave slightly higher values ( $9$ – $13$  t/ha). Another exception was found for the BioCLUST method in the  $125$ – $150$  t/ha range ( $10$  t/ha). For the mean and S.D. values calculated using the validation plot biomass values (Fig. 5b), the calculations were done only for ranges with a minimum of  $15$  plots. Otherwise, it was felt that the mean and S.D. values were not representative. For the three central ranges, i.e.,  $75$ – $100$  t/ha,  $100$ – $125$  t/ha, and  $125$ – $150$  t/ha, S.D. was similar for all methods, with values around  $5$ – $7$  t/ha. The highest S.D. values were observed for the *k*-NN method ( $12$  t/ha), in the  $>150$  t/ha range. Values for the LCC method could not be calculated for several biomass ranges because of limited ranges in the data stratum of the LCC land cover map. However, the S.D. values from the LCC method were low (between  $1.7$  and  $3$  t/ha) compared with those from the other methods (from  $4.7$  to  $13.5$  t/ha). This means that the LCC method provided a narrower range of biomass values compared with the other methods, which suggests that the LCC method may not provide sufficient representation of the real variability in biomass values observed in the landscape.

Fazakas et al. (1999) and Reese et al. (2002) suggested a scale analysis to assess the spatial variability of the error. This required the aggregation of the biomass values at different spatial resolutions from  $10$  to  $600$  ha, and averaging the RMSE

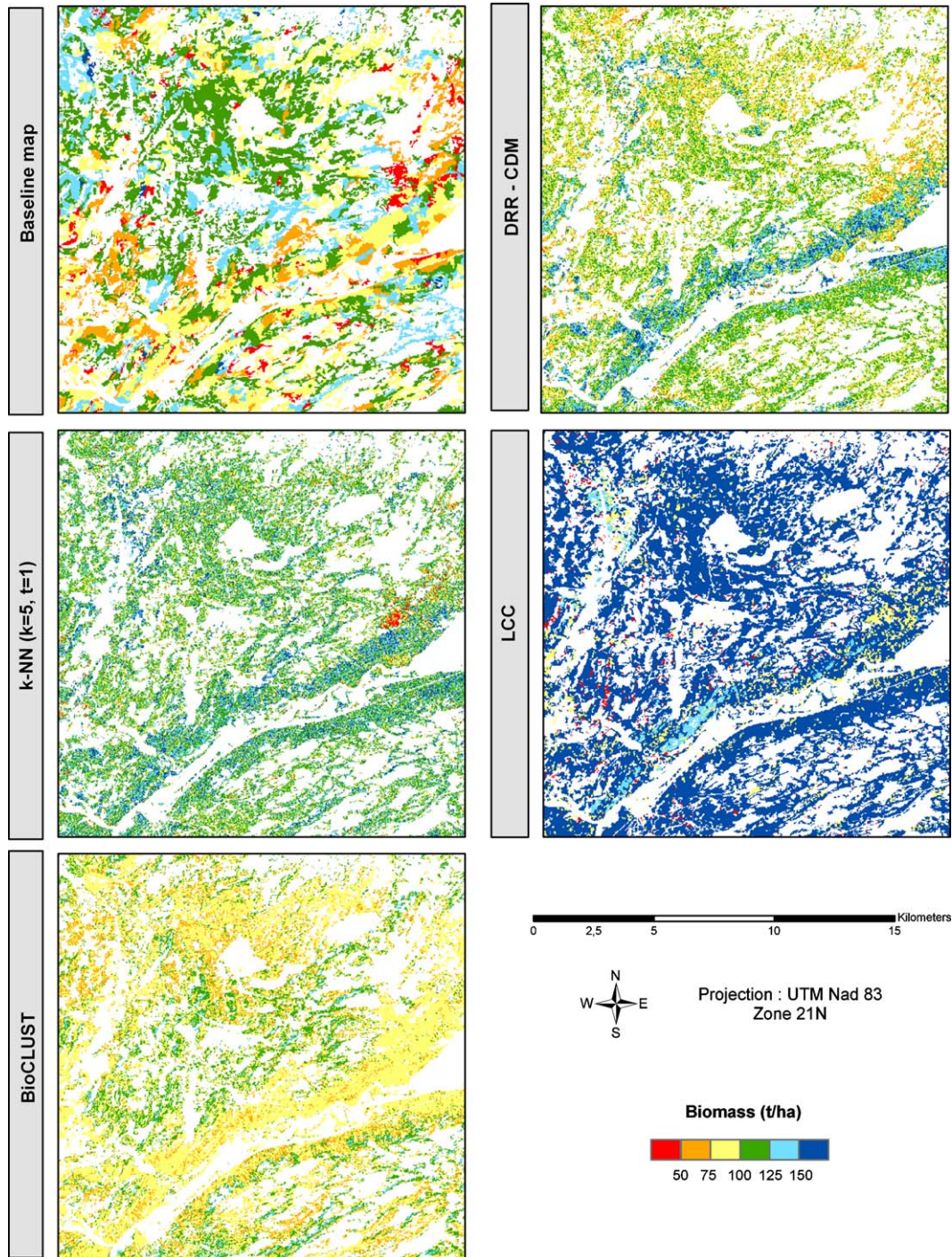


Fig. 4. Biomass maps of all methods for a section of the test area.

and bias values calculated at each aggregation level. The goal of the analysis was to identify a scale that minimizes the error. Fazakas et al. (1999) reported a significant decrease in the RMSE when the area for calculation reached 40 ha: RMSE values decrease by about 65% compared with calculations at the pixel level. These same calculations were applied on the western Newfoundland test area using the map resulting from the four methods. The spatial resolutions could range from 0.56 to 17 424 ha. Unfortunately, the results of this analysis did not lead to significant conclusions in the case of our test area. There

were not enough sample plots in the western Newfoundland test area to apply the scale analysis at a spatial resolution finer than 600 ha (2500 m × 2500 m). This problem was solved by using a regular grid superimposed on the baseline biomass map as ground truth. With such input, the RMSE values were minimized at the finest level, the pixel level (30 m). In contrast, Fazakas et al. (1999) could depend on a much larger data set of sample plots distributed more favorably in their test area. In Newfoundland, the use of the baseline map did not suggest a coarser scale where the error was minimized in the

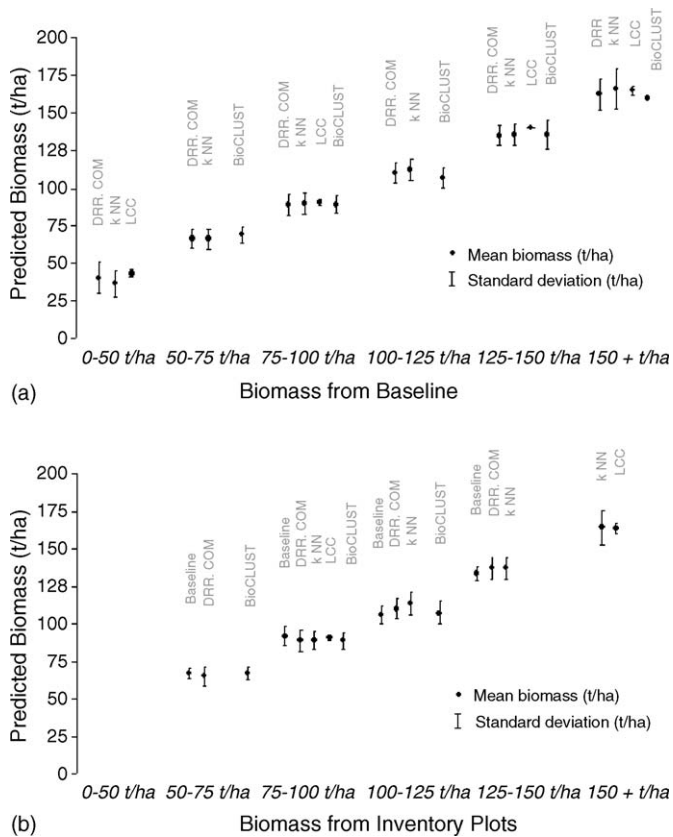


Fig. 5. Mean biomass and standard deviation for ranges of 25 t/ha for all methods, calculated (a) using the baseline map and (b) using the validation plots.

landscape. This may be due to a bias from the use of the baseline map as reference or to a very different spatial arrangement of the forest stands between the two test sites of both studies.

### 5.2. Practical aspect of each method

In selecting a method for a particular application, consideration should be given to both quantitative results and practical issues. One important practical issue is the requirement for sample plots within the image area and the requirement for precise georeferencing to allow their application. The LCC and the BioCLUST methods do not require georeferenced plots within each image. Rather, plots are only required to build the conversion tables representative of each forest stratification. Thus, the procedure is not limited by the number of available plots present in the image, which is an important advantage associated with the classification methods (LCC and BioCLUST). However, more general information on cover or species type and crown closure and/or height (as those interpreted from aerial photographs) is required for a representative area of the image. Improvement in the conversion table by including a finer stratification or by adding other relevant parameters could also improve the results, especially for the LCC method, which has the highest error of all methods.

From our experience, the most significant advantages of the  $k$ -NN method are its ability to calculate reasonable biomass values and its versatility. The  $k$ -NN method also preserves the spatial patterns of homogeneity and heterogeneity, which is not done as efficiently by the BioCLUST method, and appears to be a weakness for the LCC method. However, the requirement for georeferenced plots and the availability of a sufficient number of plots in the image are two important limitations of the  $k$ -NN. Errors in plot location will affect the spectral signature used as reference and lead to error in biomass values. Similarly, the range of real biomass values may not be mapped if the number of plots is insufficient within the spatial extent of the image. These two limitations also apply for the DRR method. Also, given that these methods rely on image-specific relationships, the transferability of these relationships to other images is not usually possible. The constraint related to the number of plots and their georeferencing will always be important in the case of the  $k$ -NN and DRR methods, in particular in the context of the Canada's forests, for which the inventory sample plots available are often very limited and variable.

Another limitation of the DRR method is the need to assess the most suited bands, vegetation indices, or band ratios for each different image. The lack of consistency in the literature and also our results suggest that it is not possible to adopt systematically a specific band or vegetation index. Finally, the DRR method requires a classification of the image corresponding to the cover or species type stratification used to build the radiometric models. Any errors generated by the classification will then lower the accuracy of the biomass estimations, as well as for the  $k$ -NN.

Overall, all four methods provide sufficiently interesting results to be considered seriously for regional mapping of biomass. From our experience, we found that choosing a method rests on both the availability of data sets required to implement a particular method and the level of precision expected for the forest ecosystems under study. In the context of the western Newfoundland test area, the BioCLUST method gave the lowest RMSE values without a requirement for georeferenced field plots specific to the image being analyzed, whereas the  $k$ -NN method provided the complex spatial patterns observed from the satellite image. However, although the LCC method gave the worst results, there may be some situations where the simplicity involved in applying the method may offset its reduced precision compared with other methods.

## 6. Conclusions

The development of a method to calculate the aboveground tree biomass fits into the Canadian-NFI strategy for forest monitoring (Gillis, 2001). In this study, four biomass mapping methods using Landsat-TM imagery were compared on a pilot region in western Newfoundland. The main conclusions arising from this study area as follows:

- Three methods (DRR,  $k$ -NN, and BioCLUST) gave similar results, with error estimations close to each other. Error calculations using the validation plots for an "All" encompassing category resulted in RMSE values of 59,

59, and 58 t/ha, respectively, and bias values of  $-8$ ,  $7$ , and  $-17$  t/ha, respectively.

- Considering the map products derived from each method and evaluated using the inventory baseline map, the BioCLUST method produced the lowest RMSE (41 t/ha) and bias ( $-4$  t/ha), followed by the DRR and  $k$ -NN methods, with RMSE values of 47 and 54 t/ha and bias values of 9 and 23 t/ha, respectively.
- The RMSE (52 t/ha) and bias ( $-6$  t/ha) calculated from the baseline map using the validation plots were lower than those reported for the remote sensing methods (DRR,  $k$ -NN, LCC, and BioCLUST). This suggests that the baseline map provided reasonable biomass estimation, from which three of the remote sensing methods are really close (DRR,  $k$ -NN, and BioCLUST).
- The BioCLUST and LCC methods are advantageous as they do not require that sample plots be within the extent of the satellite image. This facilitates enlarging the number of sample plots from relevant data sets, and does not impose a supplemental limitation on georeferenced information. The  $k$ -NN method is a practical method for biomass mapping when there are representative image-specific plot data sets available.
- The LCC method provided the least accurate results with the greatest RMSE and bias, but may be suitable when the precision of the biomass values is less critical.

## Acknowledgments

This study is included in the Earth Observation for Sustainable Development of Forests (EOSD) project supported jointly by the Canadian Space Agency and Natural Resources Canada, Canadian Forest Service. The Newfoundland Department of Forest Resources and Agrifoods provided forest inventory data sets. We thank our EOSD biomass team colleagues for their attention and follow-up on this project: R. Hall and A. Beaudoin for their useful suggestions from discussions and review of the manuscript; L. Guindon for developing the IDL program for running the  $k$ -NN algorithm; and E. Arsenault for the production of some graphs. We also thank G. Strickland for generating the EOSD Land Cover Classification and the corresponding biomass map generated by the LCC method. Thanks to the financial contribution provided by the Natural Resources Canada Science and Technology Program, the Université de Sherbrooke and the Fonds Québécois pour la Recherche sur la Nature et les Technologies which supported the work of S. Labrecque and R. Fournier.

## References

- Brown, S., Sathaye, J., Cannel, M., Kauppi, P.E., 1996. Mitigation of carbon emissions to the atmosphere by forest management. *Commonw. For. Rev.* 75 (1), 80–91.
- Brown, S.L., Schroeder, P., Kern, J.S., 1999. Spatial distribution of biomass in forests of eastern USA. *For. Ecol. Manage.* 123 (1), 81–90.
- Bérard, J., 1996. *Manuel de Foresterie*. Presses de l'Université Laval, Québec.
- Cohen, W.B., Spies, T.A., 1992. Estimating structural attributes of Douglas-fir/western hemlock forest stands from Landsat and Spot imagery. *Remote Sens. Environ.* 41 (1), 1–17.
- Dong, J., Kaufmann, R.K., Myneni, R.B., Tucker, C.J., Kauppi, P.E., Liski, J., Buermann, W., Alexeyev, V., Hughes, M.K., 2003. Remote sensing estimates of boreal and temperate forest woody biomass: carbon pools, sources and sinks. *Remote Sens. Environ.* 84, 393–410.
- Fazakas, Z., Nilsson, M., Olsson, H., 1999. Regional forest biomass and wood volume estimation using satellite data and ancillary data. *Agric. For. Meteorol.* 98–99, 417–425.
- Fournier, R.A., Luther, J.E., Guindon, L., Lambert, M.-C., Piercey, D., Hall, R.J., Wulder, M.A., 2003. Mapping above-ground tree biomass at the stand level from inventory informations: test cases in Newfoundland and Québec. *Can. J. For. Res.* 33, 1846–1863.
- Franco-Lopez, H., Ek, A.R., Bauer, M.E., 2001. Estimation and mapping of forest stand density, volume and cover type using the  $k$ -Nearest Neighbors method. *Remote Sens. Environ.* 77 (3), 251–274.
- Franklin, J., 1986. Thematic mapper analysis of coniferous forest structure and composition. *Int. J. Remote Sens.* 7 (10), 1287–1301.
- Foody, G.M., Boyd, D.S., Cutler, M.J., 2003. Predictive relations of tropical forest biomass from Landsat TM data and their transferability between regions. *Remote Sens. Environ.* 85, 463–474.
- Gerylo, G.R., Hall, R.J., Franklin, S.E., Smith, L., 2002. *Can. J. Remote Sens.* 28 (1) 68–79.
- Gillis, M.D., 2001. Canada's national forest inventory (responding to current information needs). *Environ. Mon. Assess.* 67, 121–129.
- Government of Newfoundland and Labrador, 2003. Ecoregions of Newfoundland. Forest Resources, Department of Forest Resources and Agrifoods, St. John's, NF, <http://www.gov.nf.ca/forestry/>.
- Guindon, L., Fournier, R., Luther, J.E., Hall, R.J., Arsenault, E., Piercey, D.E., Lambert, M.-C., 2002. Mapping forest biomass on several pilot regions in Canada with Landsat TM and forest inventory data. In: Proceedings of the International Geoscience and Remote Sensing Symposium and 24th Canadian Symposium on Remote Sensing (CD-ROM), Toronto, Ontario, June 24–28.
- Hall, R.J., Case, B.B., Arsenault, E., Price, D.T., Luther, J.E., Piercey, D.E., Fournier, R.A., Guindon, L., 2002. Modeling and mapping forest biomass using forest inventory and Landsat TM data: Results from the Foothills Model Forest, Alberta. In: Proceedings of the International Geoscience and Remote Sensing Symposium and 24th Canadian Symposium on Remote Sensing (CD-ROM), Toronto, Ontario, June 24–28.
- Holmström, H., 2001. Data acquisition for forestry planning by remote sensing based sample plot imputation. Doctoral dissertation. Department of Forest Resource Management and Geomatics, Swedish University of Agricultural Sciences, Umeå.
- Jakubauskas, M.E., Price, K.P., 1997. Empirical relationships between structural and spectral factors of Yellowstone lodgepole pine forests. *Photogr. Eng. Remote Sens.* 63 (12), 1375–1381.
- Katila, M., Tomppo, E., 2001. Selecting estimation parameters for the Finnish multisource National Forest Inventory. *Remote Sens. Environ.* 76 (1), 16–32.
- Labrecque, S., 2004. Cartographie de la biomasse forestière à l'aide des données de l'inventaire forestier et des images TM de Landsat. Mémoire de maîtrise. Département de géographie et télédétection, Université de Sherbrooke, Sherbrooke.
- Lavigne, M.B., 1982. Tree mass equations for common species of Newfoundland. Natural Resources Canada, Canadian Forest Service, St. John's, Nfld. Inf. Rep. N-X-213.
- Lefsky, M.A., Cohen, W.B., Spies, T.A., 2001. An evaluation of alternate remote sensing products for forestry inventory, monitoring and mapping of Douglas-fir forests in eastern Oregon. *Can. J. For. Res.* 31, 78–81.
- Luther, J.E., Fournier, R.A., Hall, R.J., Ung, C.-H., Guindon, L., Piercey, D.E., Lambert, M.-C., Beaudoin, A., 2002. A strategy for mapping Canada's forest biomass with Landsat TM imagery. In: Proceedings of the International Geoscience and Remote Sensing Symposium and the 24th Canadian Symposium on Remote Sensing (CD-ROM), Toronto, Ontario, June 24–28.
- Luther, J.E., Fournier, R.A., Piercey, D., Guindon, L., Hall, R. J., Biomass mapping using forest type and structure derived from Landsat TM imagery, *Int. J. Appl. Earth Observ. Geoinf.*, in press.
- Parresol, B.R., 1999. Assessing tree and stand biomass: a review with examples and critical comparisons. *For. Sci.* 45 (4), 573–593.

- Penner, M., Power, K., Muhairwe, C., Tellier, R., Wang, Y., 1997. Canada's forest biomass resources: deriving estimates from Canada's forest inventory. Natural Resources Canada, Canadian Forest Service, Pacific Forestry Centre, Victoria, BC, Information Report BC-X-370.
- Reese, H., Nilsson, M., Sandström, P., Olsson, H., 2002. Applications using estimates of forest parameters derived from satellite and forest inventory data. *Comput. Electron. Agric.* 37, 37–55.
- Roy, P.S., Ravan, S.A., 1996. Biomass estimation using satellite remote sensing data: an investigation on possible approaches for natural forest. *J. Biosc.* 21 (4), 535–561.
- Showengerdt, R.A., 1997. *Remote Sensing, Models, and Methods for Image Processing*, second ed. Academic Press, San Diego, CA.
- Tokola, T., 2000. The influence of fields sample data location on growing stock volume estimation in Landsat TM-based forest inventory in Eastern Finland. *Remote Sens. Environ.* 74, 422–431.
- Tokola, T., Pitkanen, J., Muinonen, E., 1996. Point accuracy of a non-parametric method in estimation of forest characteristics with different satellite materials. *Int. J. Remote Sens.* 17 (12), 2333–2351.
- Tomppo, E., Goulding, C., Katila, M., 1999. Adapting Finnish multi-source forest inventory techniques to the New Zealand preharvest inventory. *Scand. J. For. Res.* 14 (2), 182–192.
- Wood, J.E., Gillis, M.D., Goodenough, D.G., Hall, R.J., Leckie, D.G., Luther, J.E., Wulder, M.A., 2002. Earth observation for sustainable development of forests (EOSD): project overview. In: *Proceedings of the International Geoscience and Remote Sensing Symposium and the 24th Canadian Symposium on Remote Sensing (CD-ROM)*, Toronto, Ontario, June 24–28.
- Wulder, M.A., Dechka, J.A., Gillis, M.A., Luther, J.E., Hall, R.J., Beaudoin, A., Franklin, S.E., 2003. Operational mapping of the land cover of the forested area of Canada with Landsat data: EOSD land cover program. *For. Chron.* 79 (6), 1075–1083.